Effect of disorder on various physical properties of Co_2CrAl Heusler alloy films: Experiment and theory

Y. V. Kudryavtsev, V. N. Uvarov, and V. A. Oksenenko
Institute of Metal Physics, National Academy of Sciences of Ukraine, 252680 Kiev-142, Ukraine

Y. P. Lee,* J. B. Kim, and Y. H. Hyun
Department of Physics and q-Psi, Hanyang University, Seoul 133-791, Republic of Korea

K. W. Kim
Department of Physics, Sunmoon University, Asan 336-708, Republic of Korea

J. Y. Rhee
Department of Physics and BK21 Physics Research Division, Sungkyunkwan University, Suwon 440-746, Republic of Korea

J. Dubowik
Institute of Molecular Physics, Polish Academy of Sciences, 60-179 Poznań, Poland
(Received 6 October 2007; revised manuscript received 7 April 2008; published 7 May 2008)

We have investigated the effects of atomic disorder on the electronic structure and some physical properties of Co_2CrAl Heusler alloy (HA) films. Flash evaporation onto glass substrates at different temperatures (from 150 to 750 K) and postannealing at various temperatures were employed to manipulate the structural order in Co_2CrAl HA films. The $L2_1$-ordered Co_2CrAl HA films exhibit the magnetic, the transport, and the optical properties close to those of the bulk ordered sample. Increase in the structural disorder ($L2_1 \rightarrow B2 \rightarrow A2 \rightarrow$ amorphous state) causes the reduction in the saturation magnetization and the Curie temperature (T_C) down to the paramagnetic state for amorphous films. The recrystallization of amorphous Co_2CrAl HA films is accompanied by an increase in resistivity by about 10%, which is interpreted to be related to the energy gap formation at the Fermi level for the minority bands in the $L2_1/B2$-ordered state of Co_2CrAl HA. The energy-band structures of $L2_1$-ordered Co_2CrAl HA have been calculated by using an all-electron full-potential linearized-augmented-plane-wave method. The optical and the magneto-optical properties of $L2_1$-ordered Co_2CrAl HA have been experimentally investigated and explained in terms of the band structures. It was experimentally shown that the optical properties of crystalline $L2_1$ (or $B2$)-type ordered alloy at a temperature much higher than T_C do not significantly change. Structural disorder in Co_2CrAl HA from the crystalline to the amorphous state also does not radically alter the states responsible for the interband-absorption-peak formation.

DOI: 10.1103/PhysRevB.77.195104 PACS number(s): 71.20.Lp, 75.70.−i, 76.50.+g, 78.20.−e

I. INTRODUCTION

Some full Heusler alloys (HAs) of X_2YZ formula (where X and Y are $3d$ transition metals and Z is an s-p metal) are ferromagnets and are expected to exhibit 100% spin polarization (P) due to an energy-band gap for the minority-spin electrons at the Fermi level (E_F),[1–3] i.e., the so-called half-metallic property. In particular, Co-based HA have a high [above room temperature (RT)] Curie temperature (T_C) and a large magnetic moment.[4,5] Therefore, HA films are thought to be used as electrode materials for the spin-polarized current injection in spintronic devices. However, most of the HAs have not fully exhibited their unique character (i.e., the complete spin polarization at E_F) when they are incorporated into heterostructures constructed for the purposes of, for example, efficient spin injection into a semiconductor. Factors, which degrade their figure of merit, are atomic disorders, off-stoichiometry, phase separation, as well as interfacial mixing.[3,6]

Indeed, it was theoretically pointed out that the atomic disorder in full HA could reduce P.[7–9] In spite of a significant amount of theoretical[7–12] and experimental[13–23] researches, the effect of structural disorder on the electronic structures and some physical properties of HA still looks controversial.

Miura *et al.*[9] showed that the Co↔Cr disorder (i.e., the appearance of Cr atoms at the Co sites and vice versa) in Co_2CrAl HA significantly reduces the total magnetic moment and the spin polarization at E_F owing to an intense peak of the Co $3d$ states, while the Cr↔Al disorder gives practically no effect on the spin polarization. On the other hand, Co_2TiZ (Z=Al, Ga, Si, Ge, Sn, and Sb) HA behave in a different way: the Ti↔Z type of disorder remarkably degrades the half-metallicity of alloys.[8] Picozzi *et al.*[7] revealed that the Mn atoms at the Co sites in Co_2MnSi HA even result in an increase in the energy gap for the minority-spin subbands. The magnetic moment of Co_2FeAl films was found to be uninfluenced by the crystal structure.[12]

Experimentally, it has been shown that a significant disorder in amorphous Cu_2MnZ (Z=Al, In, and Sn) HA films causes spin-glass behavior at low temperatures.[17] On the other hand, it was found that amorphous Ni_2MnZ (Z=In, Ga, and Ge) (Refs. 18–20) and Cu_2MnAl (Ref. 21) HA films exhibit features of a Pauli paramagnet down to liquid helium temperatures. At the same time, amorphous Co_2MnGa HA

TABLE I. Structural properties of investigated Co_2CrAl films prepared at various deposition temperatures (T_s) and annealing temperatures (T_a). a stands for the lattice parameter, ξ for the coherence length, and δ for the mean grain size The corresponding properties of bulk Co_2CrAl alloy are shown for the comparison. The saturation magnetization (M_s) measured at 5 K is also included.

Film state	T_s (K)	T_a (K)	a (nm)	Structure	ξ (nm)	δ (nm)	M_s (emu/cm^3)
Bulk		1373	0.5726	$L2_1/B2$	51.0		311
1	150	293	0.5780	Amorphous	3.4	<2	0
2	150	538	0.5718	$A2$	35.2	?	85
3	150	608	0.5721	$B2$	24.8	$\sim$950	
4	150	760	0.5703	$L2_1/B2$	29.9	$\sim$1200	482
5	708–753		0.5702	$B2^{\star}$	22.2	20–30	363

films are ferromagnetically ordered at RT owing to the formation of Co-rich clusters.[22] Nakajima *et al.*[23] observed a very small magnetic moment (lower than $0.001\mu_B$) in Co_2MnSi amorphous films and explained this in terms of antiparallel coupling of the Co and the Mn amorphous subnetworks.

Furthermore, the interfacial properties of half metals have been investigated in detail by the first-principles calculations.[7,24,25] It was found that the Co_2CrAl compound is the only one that preserves the nearly half-metallicity at the surface, whereas in other compounds, the surface states kill the spin polarization at E_F.[24]

Miura *et al.*[9] showed that the free-energy difference between the $L2_1$- and the $B2$-type ordered unit cells for Co_2CrAl HA is one of the smallest among those for Co_2YZ HA (where Y=Ti, V, Cr, Fe, and Mn and Z=Al, Ga, Si, Ge, and Sn).[11] Therefore, Co_2CrAl HA films can be easily prepared with various degrees of order and seems to be a suitable model object for the study on the effect of structural disorder on the electronic structure and the physical properties.

It is well known that the optical and the magneto-optical (MO) properties of metals strongly depend on their electronic energy structures that are correlated with the atomic and the magnetic ordering. The correct interpretation of the experimental optical and/or MO properties of certain metals should be based on the results of the first-principles calculations of its band structure and dielectric function (DF). To the best of our knowledge, neither experimental nor theoretical studies of the optical and the MO properties of the $L2_1$-ordered Co_2CrAl HA were not carried out as well as the experimental investigation on the effect of atomic disorder on the electronic structure and the physical properties of this alloy.

In this paper, we have successfully fabricated Co_2CrAl HA films with various structural orders, and the effect of atomic disorder on the electronic structure was experimentally investigated by measuring the transport properties and by using optical and MO spectroscopy. Additionally, the energy-band structure and the DF of the $L2_1$-ordered Co_2CrAl HA have been calculated to interpret the experimental data. Furthermore, the magnetic properties were also obtained and related to the peculiarities of the electronic structure.

II. EXPERIMENTAL PROCEDURE AND THEORETICAL CALCULATIONS

Bulk Co_2CrAl HA was prepared by melting Co, Cr, and Al pieces of 99.99% purity together in an arc furnace with a water-cooled Cu hearth under an Ar atmosphere at a pressure of 1.3 atm. The Ar gas in the furnace was additionally purified by multiple melting of $Ti_{0.50}Zr_{0.50}$ alloy getter. To promote the volume homogeneity, the ingot was remelted five times and then annealed at 1373 K for 10 h in a vacuum. Weight loss after melting and annealing was not observed. The x-ray fluorescence analysis revealed an alloy composition of $Co_{0.517}Cr_{0.245}Al_{0.238}$ (hereafter, we refer to this as the bulk Co_2CrAl HA). Some physical properties of bulk Co_2CrAl alloy were investigated as reference data for studying the corresponding Co_2CrAl alloy films.

Co_2CrAl alloy films of 10×30 mm^2 in size and of about 100 nm in thickness with different degrees of structural order were simultaneously prepared by flash evaporation onto glass and NaCl substrates in a vacuum better than 2×10^{-5} Pa. Evaporation onto substrates at different temperatures T_s ($293<T_s<723$ K) and various postannealing at $293<T_a<770$ K were performed to manipulate the structural order in Co_2CrAl films. It was found that the composition of the investigated Co_2CrAl films was practically the same for all the samples and equal to $Co_{0.467}Cr_{0.281}Al_{0.246}$ (hereafter, we designate these Co_2CrAl HA films).

To obtain the Co_2CrAl films with the maximum possible disorder, we deposited them onto substrates cooled by liquid nitrogen ($T_s\approx150$ K). These as-deposited Co_2CrAl films were then subsequently annealed in series at 293 (i.e., at RT), 538, 608, and 760 K for 1 h in a high-vacuum condition. These structural states in Co_2CrAl alloy films are referred to as states 1–4 (see Table I). Additionally, some Co_2CrAl films were also deposited onto substrates at 708–753 K. This structural state is called state 5.

The structural characterization of the samples was carried out by Θ-2Θ x-ray diffraction (XRD) with Cu $K\alpha$ and Fe $K\alpha$ radiation by field-emission scanning-electron microscopy for the films deposited onto glass substrates, and by selective-area microdiffraction of transmission-electron microscopy (TEM) for the films deposited onto and separated from NaCl substrates. The structural properties of Co_2CrAl films are summarized in Table I.

The magnetic properties were investigated in a temperature range of $5 \leq T \leq 350$ K by using a superconducting quantum interference device magnetometer for samples cooled with and without external magnetic field [field-cooled (FC) and zero-field-cooled (ZFC) modes, respectively]. The temperature dependence of the out-of-plane ferromagnetic resonance (FMR) at 9.3 GHz was also measured in the 80–350 K temperature range. Additionally, the in-plane magnetic field dependence of magnetization $M(H)$ at RT was obtained by using a vibrating-sample magnetometer.

To experimentally study the influence of atomic disorder on the electronic structure of Co_2CrAl alloy, the optical and the MO [transverse Kerr effect (TKE; δ_p)] properties of films with different structural orders were measured. δ_p was measured at RT by the dynamical method using p-plane polarized light at angles of incidence of 66° and 75° in a spectral range of 240–1100 nm (5.10–1.05 eV). The optical properties [optical conductivity (OC); $\sigma = \omega\varepsilon_2/4\pi$ and ε_1, where ε_1 and ε_2 are the real and the imaginary parts of the diagonal components of DF) were obtained by using a spectroscopic rotating-analyzer ellipsometer at 150, 293, and 643 K in a spectral range of 265–2500 nm (4.7–0.5 eV) at a fixed incidence angle of 73°. The experimental values of δ_p at two angles of incidence, together with the determined values of ε_1 and ε_2, were used to calculate the off-diagonal components of DF, employing an algorithm suggested by Krinchik.[26] Additionally, the tunnel current-voltage characteristics of Co_2CrAl films have been investigated to obtain information on the density of states (DOS) near E_F. The electrical resistivity of the amorphous films was measured *in situ* in a temperature range from 150 to 750 K by employing the standard four-probe technique.

The electronic structures and both diagonal and off-diagonal components of OC tensor were calculated by using the WIEN2K package[27] by utilizing an all-electron full-potential linearized-augmented-plane-wave method.[28] For the exchange-correlation functional, the generalized-gradient-approximation version of Perdew *et al.*[29] was used. The spin-orbit coupling was included. The muffin-tin radii were determined in such a way that all the atomic spheres were almost in contact and were the same for all the atoms. We used $RK_{\max} = 8.0$, resulting in about 300 augmented plane waves as the basis functions. The detailed description of the calculational procedures for DF can be found elsewhere.[30]

III. RESULTS AND DISCUSSION

A. Transport properties

The bulk Co_2CrAl HA sample, which was used for the film deposition, had the $L2_1$ (or at least $B2$) type of order with the lattice parameter $a = 0.5727$ nm (see Fig. 1), $T_C \approx 330$ K, resistivity of 210 $\mu\Omega$ cm at RT, and the negative temperature coefficient of resistance (TCR) for 77–293 K temperature range close to those reported in the literature: $a = 0.5727 - 0.574$ nm and $T_C \approx 334$ K.[5,31] Vapor-quenching deposition onto substrates cooled by liquid nitrogen leads to the formation of highly resistive ($\rho_{293\ \mathrm{K}} \approx 200$ $\mu\Omega$ cm) amorphous state in Co_2CrAl films as evidenced by XRD and TEM results (see Fig. 2).

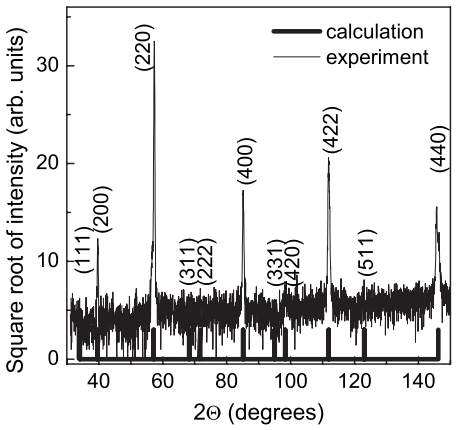

FIG. 1. Experimental XRD diffraction pattern with Fe $K\alpha$ radiation for the bulk Co_2CrAl sample, together with the calculated one for the ideal $L2_1$-ordered alloy with a lattice parameter $a = 0.5727$ nm.

It is well known that recrystallization of amorphous metal films mainly leads to a significant reduction in their resistivity.[32] However, unlike aforementioned regularity, an annealing of amorphous Co_2CrAl films causes at 590 K an abrupt increase in alloy resistivity by about 10% (see Fig. 3).

According to TEM and XRD results, crystallization of the amorphous Co_2CrAl films takes place below the anomaly in the $\rho(T)$ curve. Visual inspection of all the XRD patterns for the crystalline states 2–5 reveals only fundamental diffraction lines [among them, only the (220) diffraction line is shown in Fig. 2], while the selected-area microdiffraction TEM figures for states 3 and 5 as well as for state 4 present clear evidence for $B2$ and $L2_1$ types of order in the Co_2CrAl HA films, respectively. Interestingly, the $B2$-type ordered Co_2CrAl HA films obtained in a different way (for instance, states 3 and 5) have noticeably different mean grain sizes and probably different degrees of $B2$-type order, η (see Fig. 2). Therefore, in order to distinguish them, the structure of state

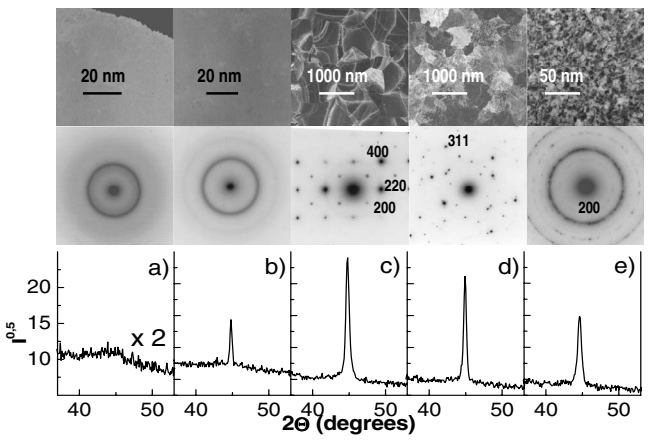

FIG. 2. Experimental TEM and XRD diffraction patterns for Co_2CrAl films deposited onto substrate cooled by liquid nitrogen and annealed at (a) 293, (b) 538, (c) 608, and (d) 728 K. All the TEM figures were obtained at the same enlargement. Column (e) shows the corresponding results for the Co_2CrAl films deposited at $T_s = 708$ K.

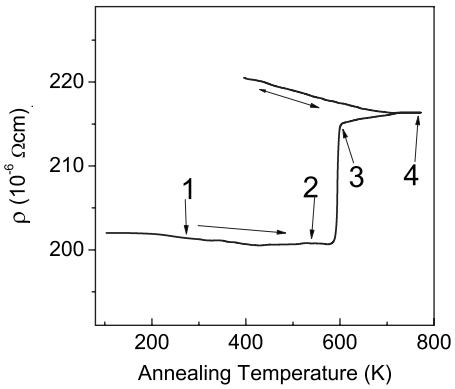

FIG. 3. Changes in the electrical resistivity $\rho(T)$ in the course of sequential heating and cooling toward RT of amorphous Co_2CrAl film. Numbers indicate the step of annealing and hence various structural states (also see Table I).

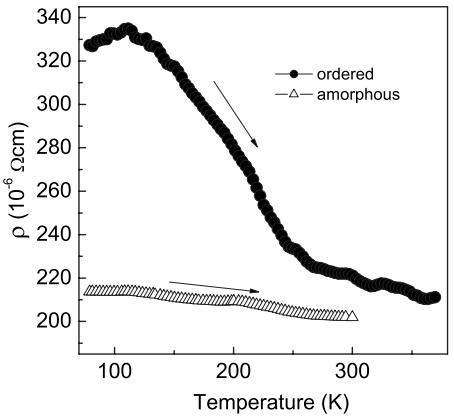

FIG. 4. Effect of temperature on the electrical resistivity $\rho(T)$ of $L2_1$-ordered and amorphous Co_2CrAl film on warming.

5 was marked as $B2^{\star}$. It can also be assumed that $\eta_3 > \eta_5$.

Structural states 1–4 in the Co_2CrAl films have been obtained after various annealing processes of the amorphous films. This is a kinetic process that leads to appearance and growth of the nuclei of new phase (phase with a higher structural order, i.e., $A2$ phase in the amorphous matrix, $B2$ phase in the $A2$ phase matrix, and so on). It is clear that, at a certain stage of annealing, the film contains a mixture of phases—parent and new phases. Therefore, the film structure shown in Table I indicates the prevailing phase. The resistivity described within the simple relaxation time τ approximation in a nearly free electron model can be expressed as

$$\rho = \frac{4\pi\gamma}{\Omega^2} = \frac{m^*\gamma}{\mathfrak{N}e^2} \approx \frac{3}{e^2 v_F^2}\frac{\gamma}{N(E_F)},$$

where $\gamma = 1/\tau$ and $\Omega = \sqrt{4\pi ne^2/m^*}$ are relaxation and plasma frequencies of free charge carriers, $\mathfrak{N}$, τ, m^*, v_F, and $N(E_F)$ are the effective concentration, the relaxation time, the mass of free charge carriers, the Fermi velocity, and the DOS at E_F, respectively.[33] Therefore, the relaxation time τ (or relaxation frequency γ) and the effective number of conduction electrons $\mathfrak{N}$ [or $N(E_F)$] are the only factors that can affect the alloy resistivity. Improvement of crystallinity of the Co_2CrAl films caused by their recrystallization should reduce scattering of free charge carriers, i.e., reduce γ (and hence ρ). It is seen that transition from state 2 to state 3 is accompanied by very significant grain-size growth (see Fig. 2). However, because of a high value of the resistivity in the amorphous state of Co_2CrAl alloy, an estimated mean free path of free-charge carriers does not exceed 1 nm. This means that a scattering at the grain boundaries for crystalline states 3 and 4 does not significantly contribute to the resulting resistivity. Thus, the only factor that can lead to an increase in the resistivity is the decrease in $N(E_F)$. This conclusion agrees with the results obtained by Miura *et al.*:[9] Co↔Cr type of disorder in Co_2CrAl alloy causes a disappearance of the energy gap for the minority-spin subbands because of the formation of an intense Co $3d$ peak at E_F.[9] At the same time, the partial DOS at E_F of Co $3d$ and Cr $3d$ states for the majority bands insignificantly reduces.[9]

We tried to obtain experimental evidence of the suggested scenario. It is well known that the optical properties of metals in the far infrared region are determined by free electrons and can be described by the Drude formulas with γ and Ω as parameters: $\varepsilon_1 = 1 - \Omega^2/(\omega^2 - \gamma^2)$, $\omega\varepsilon_2 = \Omega^2\gamma/(\omega^2 - \gamma^2)$ and $\varepsilon_1 = n^2 - k^2$, $\varepsilon_2 = 2nk$, where n and k are real and imaginary parts of complex refractive index $\tilde{N} = n - ik$. Frequency dependence of the normal reflectivity $R(\omega) = [(n-1)^2 + k^2]/[(n+1)^2 + k^2]$ in the framework of the Drude model can be easily simulated for known values of Ω and γ. Thus, possible effect of changes in Ω and γ on reflectivity in the far infrared region can be estimated. Assuming $\Omega^2 = 30 \times 10^{30}$ s^{-2} and $\gamma = 1 \times 10^{14}$ s^{-1} as starting input parameters for simulation (reasonable values for most of the metals),[33] it was shown that for these values of Ω and γ, the reflectivity for $\lambda > 5$ μm spectral range practically does not depend on the wavelength and is equal to 0.963. Two times decrease in Ω^2 (or equivalently in $\mathfrak{N}$) leads to a decrease in R down to 0.947, while two times reduction in γ must increase in $R(\omega)$ up to 0.981. Experimentally, it was shown that the reflectivity of crystalline Co_2CrAl alloy films (state 4) in the 10–18 μm spectral range is smaller than that for amorphous films by about 4% (not shown). Thus, the reflectivity measurements support the explanation of the resistivity growth based on the decrease in $N(E_F)$.

It is seen that state 3 (see Fig. 2) has at least $B2$ type of order, while state 2 exhibits only fundamental diffraction lines for XRD and TEM patterns (i.e., has $A2$ type of order). Thus, the energy gap formation at E_F induced by $A2 \rightarrow B2$ (or $L2_1$) structural transformation in Co_2CrAl alloy is thought to be the most probable origin of the observed resistivity growth. In other words, aforementioned experiments proved that the structural disorder of the $B2$ (or $L2_1$) phase down to $A2$ phase caused a resulting increase in DOS at E_F due to the disappearance of the energy gap in the minority-spin subbands.

Crystalline Co_2CrAl alloy films have a negative TCR (see Fig. 4) similar to that observed in the literature.[34,35] Such a behavior is typical for highly disordered metallic alloys whose resistivity satisfies the so-called Mooij criterion.[36] According to Mooij,[36] a material should have the negative TCR if its resistivity exceeds 150 $\mu\Omega$ cm.[37] Besides the high

level of structural disorder, negative TCR can also be caused by the charge-carrier localization.[32] Indeed, as predicted by Mott and Davis,[32] a deep gap or pseudogap in the vicinity of E_F results in localization of electrons with energy around E_F. State 4 in Co_2CrAl alloy films is characterized by the high level of order and huge grain size (see Fig. 2) Therefore, localization of charge carriers seems to be the most probable origin of negative TCR. Indeed, the Fermi level intersects the majority subbands with mainly Co 3*d* and Cr 3*d* states and highly localized 3*d* electrons provide such transport properties of alloy. Furthermore, the utmost disordered film among investigated Co_2CrAl HA films (i.e., amorphous, state 1) manifests a much lower value of negative TCR. This confirms the higher level of the charge-carrier localization in the ordered crystalline state in comparison to that of the amorphous one.

B. Magnetic properties

The magnetic properties of Co_2CrAl HA have been extensively investigated.[5,13–15] Briefly, T_C of Co_2CrAl is higher than RT ($T_C \simeq 334$ K) and the measured saturation magnetization at low temperatures has been shown[3] to be smaller than the theoretically predicted value of 3 μ_B/f.u. The experimentally determined magnetic moment ranges from 1.5 to 3 μ_B/f.u. [13,38] and is mainly localized at the Cr ($\sim 1.6\mu_B$) and the Co ($\sim 0.8\mu_B$) atoms. These values are close to our calculated results: the total calculated moment of 2.9999 μ_B/f.u. (0.8009 μ_B/Co atom and 1.5315μ_B/Cr atom). A reduced magnetization in Co_2CrAl due to the Co↔Cr antisite disorder might be a measure of this type of disorder.[9]

Although our magnetic measurements of the bulk Co_2CrAl also reveal a reduced value of magnetization of 311 emu/cm^3 as in Fig. 5(a), the low-field magnetic measurements show that its magnetic properties are more complex. The dependence of magnetization on temperature in the ZFC mode at a fixed field of 100 Oe is shown in Fig. 5(b). The magnetization increases with temperature from nearly zero to the maximum at about 250 K and then decreases to zero above $T_C \simeq 334$ K. The FC magnetization rises along the same curve (with decreasing temperature from T_C) and has an inflection at ~200 K and then levels off at low temperatures. This particular behavior of the bulk Co_2CrAl is similar to that observed in spin glass. However, since our bulk sample has a crystalline structure nominally with the $L2_1$ order (Fig. 1), the low-field magnetization characteristics are likely due to the presence of local structural disorder (for example, Co↔Cr antisite disorder) that introduces a local antiferromagnetic (AF) exchange.[9] In effect, local noncollinear spin structures can pin ferromagnetic domains in different configurations, which depend on whether the sample is cooled through the FC or the ZFC sequence.[16]

The results of FMR measurements generally agree with the static magnetic measurements. No FMR signal was detected for the amorphous Co_2CrAl films (state 1), and a faint FMR signal (~500 times smaller intensity than those from the better ordered films) was observed for the films in state 2. Figure 6 shows the temperature dependence of the FMR field

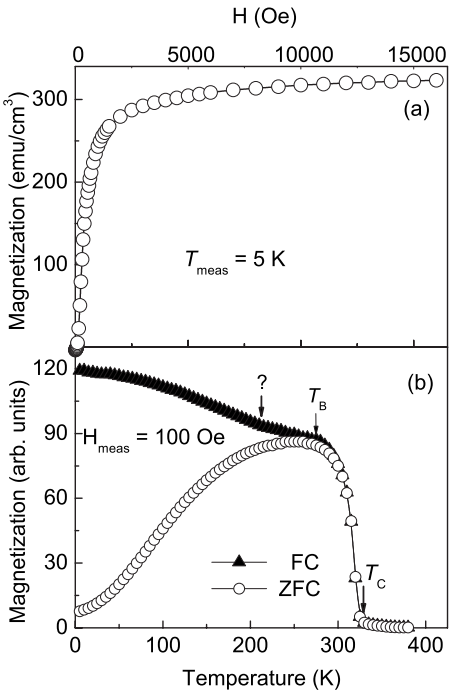

FIG. 5. (a) Magnetic field and (b) temperature dependences of magnetization for the bulk Co_2CrAl sample.

H_r (measured with a magnetic field perpendicular to the film plane) and the peak-to-peak resonance linewidth ΔH. In the perpendicular configuration, the resonance Kittel condition is particulary simple for thin magnetic films: $H_r = \omega/\gamma + 4\pi M_{\text{eff}}$, where $\omega = 2\pi f$ is angular frequency, γ is gyromagnetic factor, and $4\pi M_{\text{eff}}$ is effective magnetization. It is seen that the resonance field of the films in state 3 and, particularly, state 5 quasilinearly varies with T and the resonance field attains at $T > T_C$ a value significantly higher than $\omega/\gamma \simeq 3200$ Oe. A similar behavior at $T > T_C$ is observed for the film in state 4, which has the highest structural order. However, $H_r(T)$ of this film experiences an anomalous decrease at temperatures below 200 K and shows a clear deviation from the typical behavior (dashed curve) shown in Fig. 6(a). Such

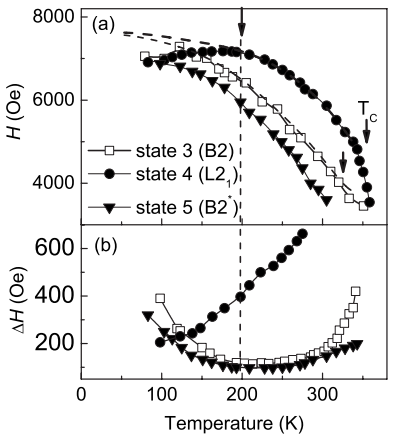

FIG. 6. Temperature dependences of (a) perpendicular resonance magnetic field and (b) FMR line width for crystalline Co_2CrAl HA films in different structural states.

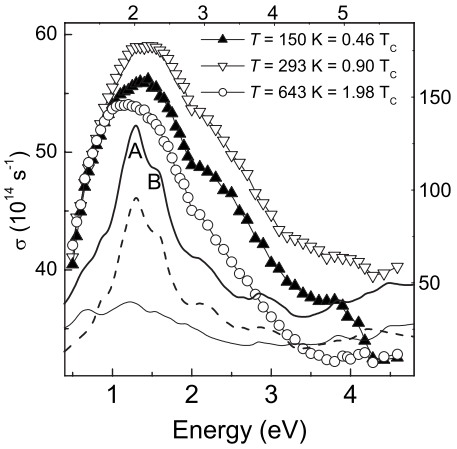

FIG. 7. Experimental (symbols) optical conductivity spectra of Co_2CrAl HA films taken below and above T_C, together with the calculated ones (lines, right and top scales). The different energy scales for experimental and calculated data are for a better comparison only in the spectral shape. Thin solid and dashed lines represent the interband contributions to the resultant optical conductivity of Co_2CrAl (thick solid line) from the majority and the minority bands, respectively.

a remarkable departure from the typical behavior was only observed for the films in state 4 and, at somewhat lower temperatures, for the films in state 5, i.e., the films with the highest structural order, and seems to have some relationship with the behavior of ZFC $M(T)$. In the perpendicular configuration, the internal magnetic field acting on the magnetization is of $\omega/\gamma \simeq 3200$ Oe for the X-band frequency of 9.08 GHz and for soft magnetic films is sufficient to saturate them. However, for the best ordered Co_2CrAl films, the field of 3000 Oe is probably too low to fully saturate them at low temperatures. This might indicate that at low temperatures, the full magnetic order is not attained in Co_2CrAl films owing to a strong pinning of the FM domains with local AF regions. The anomalous growth of ΔH below ~ 200 K [Fig. 6(b)] confirms such a scenario. FMR linewidth is a good measure of the magnetic inhomogeneities in thin films (particularly for the perpendicular configuration).[39] It is seen in Fig. 6(b) that films in states 3 and 5 have $\Delta H \approx 100$ Oe for $200 \leq T \leq 270$ K and that ΔH significantly increases at both low and high temperatures. While the increase in ΔH in the vicinity of T_C indicates the presence of spin fluctuations, the increase in ΔH at low temperatures might be due to the inhomogeneous magnetic structure. The behavior of ΔH of the film in state 3 clearly shows the presence of spin fluctuations in a very broad temperature region below T_C.

C. Optical and magneto-optical properties

Figure 7 presents the experimental OC spectra of the crystalline (at least $B2$-type ordered) Co_2CrAl alloy films (state 5) below and above T_C together with the calculated one. In the calculated OC spectrum, the Drude contribution was not included. Comparing calculated and experimental (taken at $T=150$ K) OC spectra, one can confirm a close resemblance between them in spectral shape: both OC spectra show an intense interband-absorption peak with some fine structure (marked by A and B) and a shoulder on its high-energy side. Some shift in peak position between experimental and calculated OC spectra is a typical phenomenon that originates from the problem of correct estimation of the ground state energy. Interestingly, the main contributions to the resulting OC spectrum of Co_2CrAl are formed by the electron excitations in the minority bands (see Fig. 8).

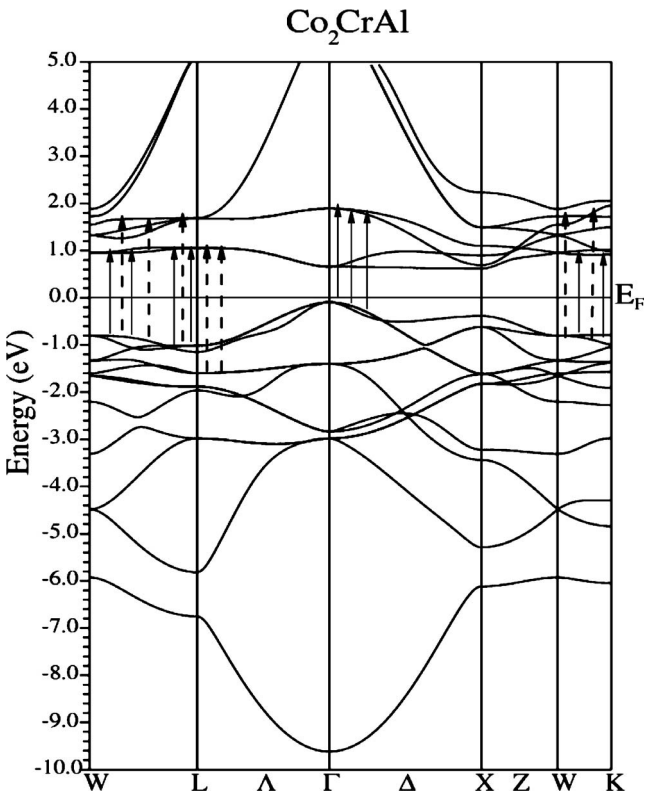

FIG. 8. Minority band structure of Co_2CrAl. Solid and dashed arrows show the most significant contributions to peak A and shoulder B, respectively, in the OC spectra.

The most intense contributions to peak A are the optical transitions from the 11th and the 12th minority bands to the 13th and the 14th minority bands and to the 15th–17th minority bands for the shoulder B. Both features have the similar **k**-space characteristics: near the K-W-L plane. These optical transitions are indicated in Fig. 9 by arrows. All the initial states involved in these transitions mostly have the Co $3d$ character with a small admixture of the Cr $3d$ and other sp characters. The 15th–17th minority bands have a considerable amount of Cr $3d$ character. Peak B has some extra contributions: interband transitions from the 8th band to the 11th and the 12th minority bands along the Γ-Δ line. Since all the bands involved in the aforementioned transitions are mostly d character, the dipole transitions are not so strong. However, both the initial and final bands are very flat or parallel to each other. Therefore, we can conclude that the joint-DOS effect is responsible for these transitions. There exist rather close similarities between the Co_2CrAl alloy and Ni_2MnIn alloy.[18] In both cases, the Co or Ni atoms play a major role in determining OC, while the Cr atom is more important in the Co_2CrAl alloy than the Mn atom in Ni_2MnIn alloy.

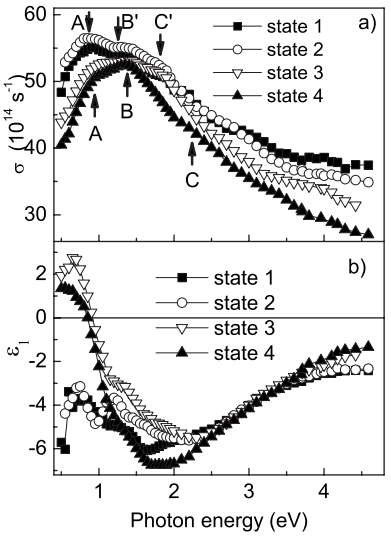

FIG. 9. Effect of the structural disorder on the optical properties of Co_2CrAl HA films.

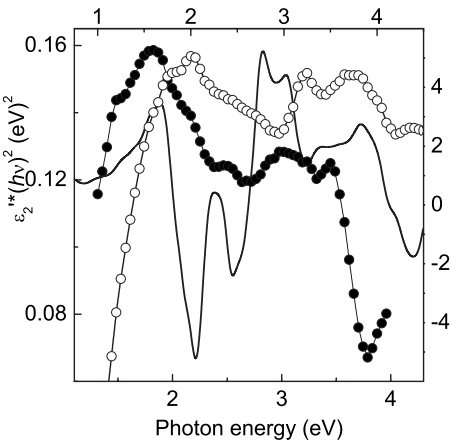

FIG. 10. Experimental (symbols) and calculated (line, right and top scales) absorptive part $\varepsilon_2'(\hbar\omega)$ of the off-diagonal components of the DF for Co_2CrAl HA films in states 4 (solid circles) and 5 (open circles). The different energy scales for experimental and calculated data are for a better comparison only in the spectral shape.

It is seen in Fig. 7 that the OC spectra for crystalline Co_2CrAl alloy films below ($T=150$ K$=0.46T_C$ and $T=293$ K$=0.90T_C$) and above T_C ($T=643$ K$=1.98T_C$) look rather similar, which insignificantly differ from each other in peak position and in smearing of the peculiarities. Redshift of the OC spectra with increasing the temperature naturally can be related to thermal lattice expansion effect.[40]

Surprisingly, nearly an invariance of the interband OC spectra below and above T_C means that the local electronic structure and/or at least the initial and final states responsible for the peaks A and B formation at $T\approx 2T_C$ look similar to those in a ferromagnetically ordered state. A similar conclusion was previously made for another Heusler alloy.[18] This also corresponds in some sense to the results of our magnetic measurements of crystalline Co_2CrAl alloy films obtained by using FMR spectroscopy.

The significant structural dependence of the optical properties of some HA has been theoretically[41] and experimentally[18–21] demonstrated. Therefore, some influence of atomic disorder on the optical properties of Co_2CrAl alloy can be expected. From the other point of view, an atomic disorder from the crystalline $L2_1$- or $B2$-type ordered state down to an amorphous one also depresses the ferromagnetic ordering in alloy at RT. This process should be accompanied by the changes in the electronic structure of alloys. Figure 9 presents the optical properties of Co_2CrAl alloy films in different structural states. The OC spectrum of mostly ordered (among investigated) Co_2CrAl alloy film exhibits an intense interband OC absorbtion peak with fine structure and a shoulder on its high-energy side. At the same time, $\varepsilon_1(\omega)$ for this sample increases in absolute value being negative with decrease in photon energy from 5 down to 2 eV. However, for $\omega<2$ eV energy region, the $\varepsilon_1(\omega)$ abruptly changes photon-energy dependence due to inclusion of intense interband absorption exhibiting the region of anomalous dispersion. Structural disorder from state 4 down to state 1 (or $L2_1/B2\rightarrow$amorphous transformation) causes visible changes in the optical properties of alloy: a magnitude of the OC in general becomes larger probably because of increase in contribution from the Drude term,[20] which is relative contribution from peak A' to the resulting OC spectrum that looks more significant; some redshifts of A'–C' peaks are observed among which peak C' is shifted most of them. At the same time, the structural disorder from state 4 down to state 1 causes significant changes in $\varepsilon_1(\omega)$ spectra that can be interpreted as a decrease in interband excitations responsible for peak A'.

We may assume that interband-absorption peaks A'–C' and peaks A–C in the OC spectra of the disordered and $L2_1/B2$-ordered states, respectively, have similar origins, since the half-metallicity of Co_2CrAl alloy film is well preserved even at the interface.[24] The increased disorder leads to the redshift of those peaks, which can be attributed to the increased lattice constant upon disordering.

The results of MO study are also in a good resemblance with the magnetic data. The MO response for amorphous state at RT is almost absent. The MO signals for crystalline Co_2CrAl alloy films with $A2$ and $B2$ types of order (states 2 and 3) are extremely weak (not shown) because of T_C's for these states are near or just below RT (see Fig. 6). At the same time, TKE spectra for $L2_1$- or $B2^*$-ordered Co_2CrAl alloy films (states 4 and 5) can be easily observed at RT. Using experimental values of $\delta_p(\omega)$ measured at two angles of incidence as well as corresponding optical constants, the dispersive $\varepsilon_1'(\omega)$ and absorptive $\varepsilon_2'(\omega)$ parts of the off-diagonal components of the DF for these Co_2CrAl alloy films have been determined. The dispersive parts demonstrate featureless, nearly linear behavior with the photon energy. Figure 10 presents the experimental and calculated $\varepsilon_2'(\omega)$ spectra for $L2_1$ and $B2^*$-type ordered Co_2CrAl alloy films. Rather good correspondence in spectral shape between the experimental and calculated $\varepsilon_2'(\omega)$ spectra can be pointed out for $L2_1$ phase. Unlike the case of the optical properties, $L2_1\rightarrow B2^*$ structural disorder effects significantly on the off-diagonal components of the DF $\varepsilon_2'(\omega)$ spectra for the state 5

is blueshifted by about 0.5 eV and somewhat smeared in comparison with that of state 4 (see Fig. 10).

IV. CONCLUSIONS

We successfully fabricated Co_2CrAl HA films with various orders by employing the flash-evaporation technique and investigated the transport, the magnetic, the optical, and the MO properties. By considering various possible factors, the energy gap formation at E_F in the $L2_1/B2$-ordered state of Co_2CrAl HA is thought to be responsible for the resistivity growth upon annealing of amorphous films. It was shown that the $L2_1$-ordered Co_2CrAl HA films are ferromagnetically ordered with a T_C close to that of the bulk sample. The increase in structural disorder of $L2_1 \rightarrow B2 \rightarrow A2 \rightarrow$amorphous state causes the reduction in T_C down to the paramagnetic state for amorphous films. The optical and the MO properties of $L2_1$-ordered Co_2CrAl HA have been experimentally investigated and explained in terms of band structure of the alloy. It was experimentally shown that the optical properties and hence the electronic band structures of crystalline $L2_1$-type ordered alloy much above T_C ($T \approx 2T_C$) are insignificantly changed. This fact suggests that the local electronic structures similar to those of ferromagnetically ordered state are conserved at $T \approx 2T_C$. The structural disorder in Co_2CrAl HA from crystalline down to amorphous state does not radically change the electronic band structure of alloy and/or, at least, the states responsible for the interband peak absorption.

ACKNOWLEDGMENTS

This work was supported by the KOSEF through Quantum Photonic Science Research Center at Hanyang University, Seoul, Korea and MEST, Korea and by KOSEF grant funded by the Korea government (MEST) (Contract No. R01-2007-000-20974-0). This work was also supported by the Korea Research Foundation grant funded by the Korean Government (MOEHRD) (Contract No. KRF-2005-005-J11903). This work was also supported under Grant No. 27/07-H funded by National Academy of Sciences of Ukraine (NAS of Ukraine).

*Corresponding author; yplee@hanyang.ac.kr

[1] S. Ishida, S. Sugimura, S. Fujii, and S. Asano, J. Phys.: Condens. Matter **3**, 5793 (1991).
[2] S. Fujii, S. Sugimura, S. Ishida, and S. Asano, J. Phys.: Condens. Matter **2**, 8583 (1990).
[3] I. Galanakis, P. H. Dederichs, and N. Papanikolaou, Phys. Rev. B **66**, 174429 (2002).
[4] P. J. Webster, Contemp. Phys. **10**, 559 (1969).
[5] K. H. J. Buschow, P. G. van Engen, and R. Jongebreur, J. Magn. Magn. Mater. **38**, 1 (1983), and references therein.
[6] K. Nagao, Y. Miura, and M. Shirai, Phys. Rev. B **73**, 104447 (2006).
[7] S. Picozzi, A. Continenza, and A. J. Freeman, Phys. Rev. B **69**, 094423 (2004).
[8] S. C. Lee, T. D. Lee, P. Blaha, and K. Schwartz, J. Appl. Phys. **97**, 10C307 (2005).
[9] Y. Miura, K. Nagao, and M. Shirai, Phys. Rev. B **69**, 144413 (2004).
[10] D. Orgassa, H. Fujiwara, T. C. Schulthess, and W. H. Butler, Phys. Rev. B **60**, 13237 (1999).
[11] Y. Miura, M. Shirai, and K. Nagao, J. Appl. Phys. **99**, 08J112 (2006).
[12] N. Tezuka, S. Okamura, A. Miyazaki, M. Kikuchi, and K. Inomata, J. Appl. Phys. **99**, 08T314 (2006).
[13] H. J. Elmers, G. H. Fecher, D. Valdaitsev, S. A. Nepijko, A. Gloskovskii, G. Jakob, G. Schönhense, S. Wurmehl, T. Block, C. Felser, P.-C. Hsu, W.-L. Tsai, and S. Cramm, Phys. Rev. B **67**, 104412 (2003).
[14] A. Husmann and L. J. Singh, Phys. Rev. B **73**, 172417 (2006).
[15] C. Felser, H. J. Elmers, and G. H. Fecher, in *Half Metallic Alloys*, edited by I. Galanakis and P. H. Dederichs (Springer, New York, 2005), p. 113.
[16] T. Krenke, M. Acet, E. F. Wassermann, X. Moya, L. Mañosa, and A. Planes, Phys. Rev. B **72**, 014412 (2005).
[17] L. Krusin-Elbaum, A. P. Malozemoff, and R. C. Taylor, Phys. Rev. B **27**, 562 (1983).
[18] Y. V. Kudryavtsev, Y. P. Lee, and J. Y. Rhee, Phys. Rev. B **69**, 195104 (2004).
[19] Y. V. Kudryavtsev, Y. P. Lee, and J. Y. Rhee, Phys. Rev. B **66**, 115114 (2002).
[20] V. A. Oksenenko, L. N. Trofimova, Yu. N. Petrov, Y. V. Kudryavtsev, J. Dubowik, and Y. P. Lee, J. Appl. Phys. **99**, 063902 (2006).
[21] Y. V. Kudryavtsev, V. A. Oksenenko, N. N. Lee, Y. P. Lee, J. Y. Rhee, and J. Dubowik, J. Appl. Phys. **97**, 113903 (2005).
[22] Y. V. Kudryavtsev, V. A. Oksenenko, V. A. Kulagin, J. Dubowik, and Y. P. Lee, J. Magn. Magn. Mater. **310**, 2271 (2007).
[23] K. Nakajima, G. Fen, C. Caillol, L. S. Dorneles, M. Venkatesan, and J. M. D. Coey, J. Appl. Phys. **97**, 10C904 (2005).
[24] I. Galanakis, J. Phys.: Condens. Matter **14**, 6329 (2002).
[25] I. Galanakis, M. Lezaić, G. Bihlmayer, and S. Blügel, Phys. Rev. B **71**, 214431 (2005).
[26] G. S. Krinchik, *Physics of Magnetism* (MGU, Moscow, 1976) (in Russian).
[27] P. Blaha, K. Schwarz, G. K. H. Madsen, D. Kvasnicka, and J. Luitz, *WIEN2k, An Augmented Plane Wave Plus Local Orbitals Program for Calculating Crystal Properties* (Karl-heinz Schwarz, Technical Universität Wien, Austria, 2001).
[28] E. Wimmer, H. Krakauer, M. Weinert, and A. J. Freeman, Phys. Rev. B **24**, 864 (1981).
[29] J. P. Perdew, K. Burke, and M. Ernzerhof, Phys. Rev. Lett. **77**, 3865 (1996).
[30] J. Y. Rhee, J. Korean Phys. Soc. **43**, 792 (2003).
[31] M. Zhang, Z. Liu, H. Hu, G. Liu, Y. Cui, J. Chen, G. Wu, X. Zhang, and G. Xiao, J. Magn. Magn. Mater. **277**, 130 (2004).
[32] N. F. Mott and E. A. Davis, *Electron Processes in Non-Crystalline Materials* (Clarendon, Oxford, 1971), Vol. I.
[33] M. M. Noskov, *Optical and Magnetooptical Properties of Met-*

als (Ural Scientific Center, USSR, 1983).
[34] R. Kelekar and B. M. Clemens, J. Appl. Phys. **96**, 540 (2004).
[35] A. Hirohata, H. Kurebayashi, H. S. Okamura, M. Kikuchi, T. Masaki, T. Nozaki, N. Tezuka, and K. Inomata, J. Appl. Phys. **97**, 103714 (2005).
[36] S. Dugdale, *The Electrical Properties of Disordered Metals* (Cambridge University Press, Cambridge, 1995).
[37] J. H. Mooij, Phys. Status Solidi A **17**, 521 (1973).
[38] T. Block, M. J. Carey, B. A. Gurney, and O. Jepsen, Phys. Rev. B **70**, 205114 (2004).
[39] J. Dubowik, Y. V. Kudryavtsev, and Y. P. Lee, J. Appl. Phys. **95**, 2912 (2004).
[40] Y. P. Lee, K. W. Kim, J. Y. Rhee, Y. V. Kudryavtsev, and V. V. Nemoshkalenko, Phys. Rev. B **60**, 8067 (1999).
[41] J. F. Wan and J. N. Wang, Physica B **355**, 172 (2005).